

Scaling the Depressurization Behavior of Fluids in Phase Equilibria

José N. Reyes, Jr.

Department of Nuclear Engineering
Oregon State University
116 Radiation Center
Corvallis, OR 97331-5902, USA
FAX: 541-737-4678

ABSTRACT

In this paper, I briefly summarize the rationale for scaling the depressurization behavior of fluids in phase equilibria. I begin by developing a simple depressurization rate equation from the control volume mass and energy balance equations. The depressurization rate equation is then presented in dimensionless form and an order of magnitude analysis is performed using the conditions expected for the Westinghouse Advanced Passive 600 MW(e) nuclear power plant. I then demonstrate that the key property group governing the depressurization rate exhibits "self-similarity" over a wide range of pressures. To assess the validity of the scaling approach, I compare the test results for a counterpart test performed both in the full pressure SPES facility in Piacenza, Italy and the reduced pressure APEX facility at the Oregon State University in Corvallis, Oregon.

I. INTRODUCTION

The analysis of the depressurization behavior of nuclear reactor systems following postulated piping ruptures has been the focus of numerous safety studies. Because of the significant expense involved in testing the safety systems of full-scale nuclear power plants, the use of reduced scale test facilities offers a significant economic advantage. Scaled integral system facilities such as the Rig of Safety Assessment (ROSA) in Japan, and the Loss of Fluid Test (LOFT) in the United States and scaled separate effects tests have been successfully used for many years to study a variety of phenomena. As part of the certification effort for the AP600, Westinghouse and the U.S. Department of Energy recently developed the Advanced Plant Experiment (APEX) at Oregon State University. One of the interesting aspects of this facility was the use of pressure scaling to simulate the behavior of portions of AP600 depressurization

transients. The purpose of this paper is to summarize the basis for pressure scaling and the constraints associated with its application (Reyes, et. al. [1]).

II. CONSERVATION EQUATIONS

Let us begin our examination of depressurization behavior with the fluid mass and energy conservation equations. The mass conservation equation is given by:

$$\frac{dM}{dt} = \dot{m}_{in} - \dot{m}_{out} \quad (1)$$

where M is the fluid mass within the control volume and \dot{m} represents the mass flow rate entering or leaving the control volume.

The energy conservation equation for the fluid is expressed as follows:

$$\frac{dU}{dt} = (\dot{m}h)_{in} - (\dot{m}h)_{out} + \dot{q}_{Net} - P \frac{dV}{dt} \quad (2)$$

where U is the internal energy of the fluid within the control volume, h is the enthalpy of the fluid entering or leaving the control volume, \dot{q}_{Net} is the net energy into the system; P is the system pressure and V is the system volume.

The specific internal energy and the specific volume are defined respectively as follows:

$$e = \frac{U}{M} \quad (3)$$

$$v = \frac{V}{M} \quad (4)$$

The total change in specific internal energy can be written in terms of partial differentials with respect to pressure and specific volume as follows:

$$de = \left(\frac{\partial e}{\partial p} \right)_v dp + \left(\frac{\partial e}{\partial v} \right)_p dv \quad (5)$$

Substituting equation (3) into (2) yields:

$$\frac{dMe}{dt} = (\dot{m}h)_{in} - (\dot{m}h)_{out} + \dot{q}_{Net} - P \frac{dV}{dt} \quad (6)$$

Expanding the first term on the LHS of equation (6), substituting equation (1) and rearranging yields:

$$M \frac{de}{dt} = \dot{m}_{in} (h_{in} - e) - \dot{m}_{out} (h_{out} - e) + \dot{q}_{Net} - P \frac{dV}{dt} \quad (7)$$

Substituting equation (5) into (7), and rearranging yields:

$$M \left(\frac{\partial e}{\partial p} \right)_v \frac{dp}{dt} = \dot{m}_{in} (h_{in} - e) - \dot{m}_{out} (h_{out} - e) + \dot{q}_{Net} - P \frac{dV}{dt} - M \left(\frac{\partial e}{\partial v} \right)_p \frac{dv}{dt} \quad (8)$$

Using equation (4), and the mass conservation equation, the last term on the RHS of equation (8) is written as:

$$M \left(\frac{\partial e}{\partial v} \right)_p \frac{dv}{dt} = \left(\frac{\partial e}{\partial v} \right)_p \frac{dV}{dt} - v \left(\frac{\partial e}{\partial v} \right)_p (\dot{m}_{in} - \dot{m}_{out}) \quad (9)$$

Substituting back into equation (8) yields:

$$M \left(\frac{\partial e}{\partial p} \right)_v \frac{dp}{dt} = \dot{m}_{in} \left[h_{in} - e + v \left(\frac{\partial e}{\partial v} \right)_p \right] - \dot{m}_{out} \left[h_{out} - e + v \left(\frac{\partial e}{\partial v} \right)_p \right] + \dot{q}_{Net} - \left[P + \left(\frac{\partial e}{\partial v} \right)_p \right] \frac{dV}{dt} \quad (10)$$

which is the "depressurization rate equation." For a control volume with rigid boundaries, which is typically the case, equation (10) becomes:

$$M \left(\frac{\partial e}{\partial p} \right)_v \frac{dp}{dt} = \dot{m}_{in} \left[h_{in} - e + v \left(\frac{\partial e}{\partial v} \right)_p \right] - \dot{m}_{out} \left[h_{out} - e + v \left(\frac{\partial e}{\partial v} \right)_p \right] + \dot{q}_{Net} \quad (11)$$

Equation (11) shall provide the basis for scaling the depressurization behavior.

III. SCALING METHODOLOGY

The Hierarchical Two-Tiered Scaling (H2TS) methodology (Zuber [2]) was used to scale the APEX facility. The basic objective of the H2TS methodology is to develop sets of characteristic time ratios, (i.e., Π groups), for the important transfer processes. This is done by casting the governing control volume balance equations in dimensionless form. That is, each term of a governing equation is divided by its respective initial condition. Hence all of the terms are normalized to range between zero and unity. The equation is further normalized relative to the expected dominant transport process which defines the time scale for the transient phenomenon of interest.

Physically, each characteristic time ratio (Π_i) is composed of a specific frequency (ω_i), which is an attribute of the specific transport process, and the residence time constant for the control volume, (τ_{cv}). That is:

$$\Pi_i = \omega_i \tau_{cv} \quad (12)$$

The specific frequency defines the mass, momentum or energy transfer rate for a particular process. The residence time defines the total time available for the transfer process to occur within the control volume. A numerical value of $\Pi_i \ll 1$, means that only a small amount of the conserved property would be transferred in the limited time available for the specific process to evolve.

As a result, the specific process would not be important to the overall transient. Numerical values of $\Pi_i \geq 1$ means that the specific process evolves at a high enough rate to permit significant amounts of the conserved property to be transferred during the time period (τ_{cv}). Such a process would be important to the overall transient behavior.

In general, by writing each Π group in terms of a model (reduced scale) to prototype (full scale) ratio and setting the ratio to unity, a similarity criterion is developed. That is:

$$\Pi_R = 1 \quad (13)$$

The geometric or operating parameters are then adjusted to satisfy the criterion.

The scaling approach described in this section shall now be applied to equations (1) and (11) to obtain the characteristic time ratios and a residence time constant for the depressurization process.

IV. CHARACTERISTIC TIME RATIOS AND ORDER OF MAGNITUDE ANALYSIS

The mass conservation equation, equation (1), can be expressed in dimensionless form by dividing each term by its respective initial condition and further dividing by the mass flow rate of the fluid leaving the break. This results in the following dimensionless mass balance equation:

$$\tau_{\text{sys}} \frac{dM^+}{dt} = \Pi_m \dot{m}_{\text{in}}^+ - \dot{m}_{\text{out}}^+ \quad (14)$$

where the superscript "+" terms indicate normalization with respect to initial conditions. The residence time constant, (τ_{sys}), for the depressurization transient is given by:

$$\tau_{\text{sys}} = \frac{M_0}{\dot{m}_{\text{out},0}} \quad (15)$$

and the characteristic time ratio is given by:

$$\Pi_m = \frac{\dot{m}_{\text{in},0}}{\dot{m}_{\text{out},0}} \quad (16)$$

Π_m is the system mass flow rate ratio. For a constant injection flow rate, Π_m represents the total liquid mass injected into the control volume during the residence time (τ_{sys}).

Equation (11) can be expressed in dimensionless form by dividing each term by its respective initial condition and further dividing both sides of the equation by the fluid energy flow rate initially leaving the break. This results in the following dimensionless energy balance equation:

$$\begin{aligned} \epsilon_o M^+ \left(\frac{\partial e}{\partial P} \right)_v \frac{dP^+}{dt} = & \Pi_h \dot{m}_{\text{in}}^+ \left[h_{\text{in}} - e + v \left(\frac{\partial e}{\partial v} \right)_p \right]_{p_{j,0}} \\ & - \dot{m}_{\text{out}}^+ \left[h_{\text{out}} - e + v \left(\frac{\partial e}{\partial v} \right)_p \right] \\ & + \Pi_\Gamma \dot{q}_{\text{Net}}^+ \end{aligned} \quad (17)$$

The characteristic time ratios are given by the following:

$$\Pi_h = \frac{\dot{m}_{\text{in},0} \left[h_{\text{in}} - e + v \left(\frac{\partial e}{\partial v} \right)_p \right]_{p_{j,0}}}{\dot{m}_{\text{out},0} \left[h_{\text{out}} - e + v \left(\frac{\partial e}{\partial v} \right)_p \right]_{p_{j,0}}} \quad (18)$$

$$\Pi_\Gamma = \frac{\dot{q}_{\text{Net},0}}{\dot{m}_{\text{out},0} \left[h_{\text{out}} - e + v \left(\frac{\partial e}{\partial v} \right)_p \right]_{p_{j,0}}} \quad (19)$$

Π_h is the energy flow rate ratio. It represents the ratio of the total energy change due to fluid injection to that lost by the break flow during the residence time (τ_{sys}). Π_Γ is the power ratio. For a fluid mixture at saturated conditions, it represents the total vapor mass generated in the primary system during the residence time (τ_{sys}).

The key fluid property for the depressurization process is the volumetric dilation, ϵ_o . It is given by:

$$\epsilon_o = \frac{P_o \left(\frac{\partial e}{\partial P} \right)_{v,0}}{\left[h_{\text{out}} - e + v \left(\frac{\partial e}{\partial v} \right)_p \right]_{p_{j,0}}} \quad (20)$$

Equation (20) reveals that the volumetric dilation couples the system intensive energy change to the intensive energy at the break. For high pressure systems venting to the ambient, the fluid properties at the break are determined at critical flow conditions. Therefore, h_{out} equals h_{out}^* ; where the superscript denotes critical flow conditions.

For saturated mixtures it can be shown that:

$$\epsilon_o = f \left(\alpha, \frac{Pv_{fg}}{h_{fg}} \right) \quad (21)$$

To determine which of the transport processes are most important to a depressurization transient and consequently which parameters should be scaled in the test facility, an order of magnitude analysis is performed. Figure 1 presents the numerical values for the characteristic time ratios presented above as evaluated for AP600 conditions. The

characteristic time ratios have been evaluated at 5 percent and 3 percent decay power using both the Henry-Fauske [3] and Homogeneous Equilibrium critical flow models to estimate the break flow rates at saturated liquid conditions. The figure indicates that for break diameters greater than approximately 5 cm (~2 inches), the depressurization process is dominated by the mass flow rate leaving the system through the break. That is, the values for Π_b and Π_T are much smaller than unity. However, as the break diameters decrease, these two Π groups become increasingly important and the depressurization behavior is dominated by the volumetric expansion within the control volume.

AP600 DEPRESSURIZATION RATE EQUATION

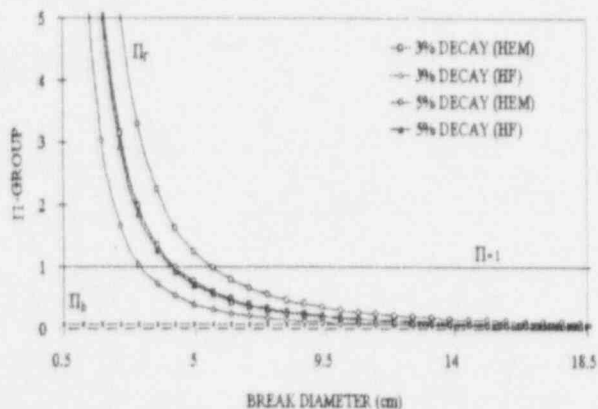


Figure 1. Order of Magnitude Analysis for the Depressurization Rate Equation Dimensionless Groups

Thus, for scaling the depressurization behavior associated with breaks smaller than 1.25 cm (1 inch), the characteristic time ratios associated with the energy equation are most important. However, for scaling the depressurization behavior associated with breaks larger than 5 cm (2 inches), scaling the break mass flow rate is most important.

V. SELF-SIMILARITY OF SATURATED FLUID PROPERTIES

The success of scaling depressurization behavior in reduced pressure test facilities ultimately lies in the fact that several properties of fluids in phase equilibria exhibit "self-similarity" over a wide range of conditions. As explained by Briggs and Peat [4] in their discussion on Mandelbrot fractals, self-similarity is a "repetition of detail at descending scales." I have found this to be true for the following important property group.

The ratio of the pressure work associated with phase change to the total energy associated with phase change can be written as follows:

$$\psi = \frac{P v_{fg}}{h_{fg}} \quad (22)$$

where P is the saturation pressure, v_{fg} is the change in specific volume and h_{fg} is the latent heat of vaporization. Note that the volumetric dilation for saturated mixtures depends on this group. If one graphs this quantity against the corresponding saturation temperature a linear trend is observed beginning at the triple point temperature, T_t , and extending nearly to the critical point temperature, T_c . The saturation temperature can be expressed as a dimensionless quantity as follows:

$$\theta = \frac{T - T_t}{T_c - T_t} \quad (23)$$

Figure 2 presents a graph of ψ versus θ for water at saturated conditions (Irey, et. al. [5] Keenan, et al. [6]). This figure illustrates that the data is quite linear for the range of dimensionless temperatures given by:

$$0 \leq \theta \leq 0.8 \quad (24)$$

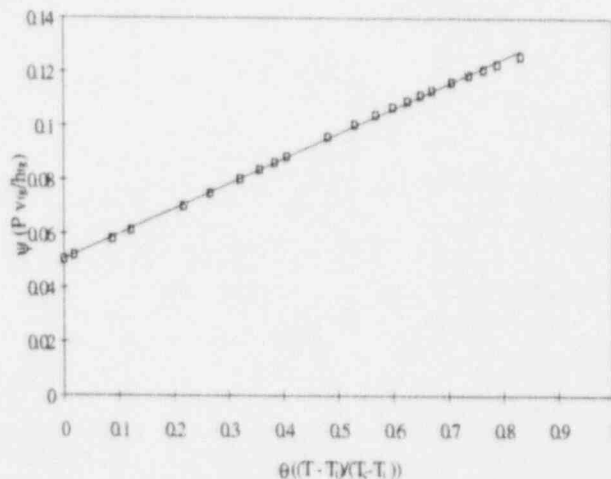


Figure 2. Graph of Dimensionless Fluid Property ψ for Water

As the critical point is approached, for values of θ greater than 0.8, the trend becomes non-linear. The intercept is the value of ψ evaluated at the triple point. That is:

$$\psi(0) = \psi_t \quad (25)$$

The slope is a constant given by:

$$\frac{d\psi}{d\theta} = c_1 \quad (26)$$

Numerous fluids display the same trend as observed in Figure 2 and can be plotted on a single graph in terms of $(\psi - \psi_t)$ versus θ .

Based on the results, the equation relating ψ and θ is given by:

$$\psi = c_i \theta + \psi_i \quad (27)$$

For water, c_i equals 0.0926 and ψ_i equals 0.05038.

1. Equation of State for Saturated Pressure and Temperature

The Clausius-Clapeyron equation is the classical differential equation that defines the slope dP/dT for a phase equilibrium curve. It is derived by assuming that the Gibb's free energies for the two phases being considered are equal, e.g., Lay, J.E. [7]. Using the standard definition for the Gibb's free energy and relating the change in entropy to the latent heat of vaporization and the saturation temperature yields the well-known Clausius-Clapeyron equation:

$$\frac{dP}{dT} = \frac{h_{fg}}{v_{fg} T} \quad (28)$$

The Clausius-Clapeyron equation can be used with equation (27) to obtain an equation of state for the saturation pressure and temperature. Let us rewrite equation (27) as follows:

$$\frac{P v_{fg}}{h_{fg}} = bT + a \quad (29)$$

where

$$a = \psi - bT_i \quad (30)$$

Rearranging equation (29) yields:

$$\frac{h_{fg}}{v_{fg}} = \frac{P}{(bT + a)} \quad (31)$$

where:

$$b = \frac{c_i}{(T_c - T_i)} \quad (32)$$

Substituting equation (31) into the Clausius-Clapeyron equation yields:

$$\frac{dP}{dT} = \frac{P}{T(bT + a)} \quad (33)$$

Separating the variables and integrating both sides yields an equation of state for saturation pressure in terms of saturation temperature. That is:

$$\int_{P_i}^P \frac{dP}{P} = \int_{T_i}^T \frac{dT}{T(bT + a)} \quad (34)$$

the solution of which is:

$$P = P_i \left[\left(\frac{a + bT_i}{a + bT} \right) \left(\frac{T}{T_i} \right) \right]^{\frac{1}{a}} \quad (35)$$

Where P_i and T_i are the saturation pressure and temperature at the triple point respectively. Equation (35) is the state equation that relates saturation pressure to saturation temperature.

Comparisons of equation (35) to tabulated values of saturation pressure and temperature of various fluids indicates excellent agreement; having R^2 values greater than 0.994.

2. Scaled Processes Using Similar Fluids in Phase Equilibria

Let us now turn our attention to the problem of relating the saturation pressure and temperature in a reduced pressure test model to the same properties in a full pressure prototype. Let us suppose that the same working fluid is used in the model as in the prototype. We would need to relate the fluid properties in the full pressure plant to those in the reduced pressure model. If we assume that the depressurization process evolves along the saturation curve, then equation (35) is directly applicable.

Equation (35) has been normalized using the saturation pressure and temperature corresponding to the triple point of the fluid. However, the saturation pressure and temperature corresponding to any point between θ equal to zero and 0.8 would serve equally well. For depressurization processes, it is convenient to select the initial saturation pressure and temperature as the "reference" parameters. Thus, equation (35) becomes:

$$P = P_o \left[\left(\frac{a + bT_o}{a + bT} \right) \left(\frac{T}{T_o} \right) \right]^{\frac{1}{a}} \quad (36)$$

where the subscript "o" denotes a reference property evaluated at the initial saturated equilibrium conditions and

the constants "a" and "b" are as defined previously. Equation (36) can be written as a scaling ratio as follows:

$$\left(\frac{P}{P_o}\right)_R = \left[\left(\frac{a + bT_o}{a + bT}\right)_R \left(\frac{T}{T_o}\right)_R\right]^{\frac{1}{a}} \quad (37)$$

where the subscript "R" denotes the ratio of model to plant properties. Because the same fluid is used in both cases, the coefficients a and b are identical in the model and the plant.

Substituting equation (29) into (37) and rearranging yields:

$$\left(\frac{P}{P_o}\right)_R = \left[\frac{(h_{fg} T/v_{fg})}{(h_{fg} T/v_{fg})_o}\right]^{\frac{1}{a-1}} \quad (38)$$

Figure 3 reveals that the right-hand side of equation (38) is essentially unity for all values of pressure ratios (P/P_o) in the model and the prototype. Thus:

$$\left[\frac{(h_{fg} T/v_{fg})}{(h_{fg} T/v_{fg})_o}\right] = 1 \quad (39)$$

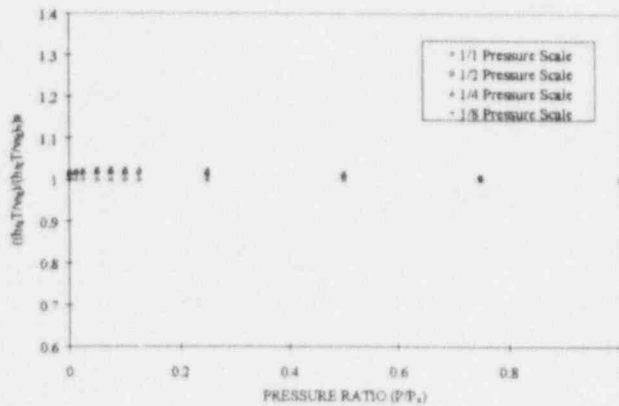


Figure 3. Effect of Pressure Scaling on the Term on the Right-hand Side of Equation (38)

Substituting this result into equation (38) yields:

$$\left(\frac{P}{P_o}\right)_R = 1 \quad (40)$$

or in terms of model parameters, denoted by the subscript "m" and the plant parameters, denoted by the subscript "p",

$$P_p = \left(\frac{P_{o,p}}{P_{o,m}}\right) P_m \quad (41)$$

Equation (41) relates the saturation pressure in the model to the saturation pressure in the plant. This same result can be obtained using the graphical approach presented by Kocamustafogullari and Ishii [8].

Substituting equation (40) into (37) yields an equation that can be used to relate the saturation temperatures in the model to those of the plant. After some algebra, one obtains:

$$T_p = \frac{a}{\left(\frac{(a + bT)_m (T_o)_R}{T_m (a + bT_o)_R} - b\right)} \quad (42)$$

The results herein are applicable to the range of dimensionless temperatures, θ , between zero and 0.8. Equation (35) presents a state equation that relates saturation pressure to saturation temperature.

Equations (41) and (42) relate the saturation pressures and temperatures of a reduced pressure scale model to those of a full pressure prototype. This allows direct data comparisons when the process being examined evolves along the phase equilibrium curve.

The property of "self-similarity" is demonstrated by equations (39) and (40). That is, any continuous subset of these fluid properties can be scaled by a single constant to re-create a "scaled" set of fluid properties applicable to a wider range of pressures.

VII. COMPARISONS OF A SPES AND APEX DEPRESSURIZATION TRANSIENT

Counterpart tests have been performed in the SPES and APEX test facilities (Hochreiter and Reyes [9]). These tests provide points of comparison for the facilities which enable one to understand scaling and operating differences. This section examines a 2-inch small break loss of coolant accident. Table 1 presents the general scaling ratios for the test facilities relative to the full-scale AP600.

| Table 1 | | |
|----------------------|-------|--------|
| Scaling Ratios | APEX | SPES-2 |
| Lengths | 1:4 | 1:1 |
| Relative Elevations | 1:4 | 1:1 |
| Flow Areas | 1:48 | 1:395 |
| Volumes | 1:192 | 1:395 |
| Decay Power | 1:96 | 1:395 |
| Fluid Velocity | 1:2 | 1:1 |
| Fluid Transient Time | 1:2 | 1:1 |
| Mass Flow Rate | 1:96 | 1:395 |

*Note: Ratios are relative to the full-scale AP600

Scaling factors will need to be applied to the APEX and SPES-2 results to compare time, pressure, and flowrates. The APEX time scale must be multiplied by a factor of two and its pressure scale normalized using the reference pressure (maximum pressure on secondary side). Similarly, the SPES-2 pressure scale can also be normalized using the reference pressure for the test. The flow rate normalization factor in SPES-2 is the maximum flow rate for the process being examined. For example, the maximum accumulator injection flow observed. For purposes of comparison, the flow rate normalization factor in APEX would be the maximum flow rate observed for the identical process in SPES-2 multiplied by the ratio 395/96. Thus, the flowrates can be compared on a similar basis.

A 2-inch cold leg break was simulated in both the APEX and SPES-2 facilities. The break location for these tests was at the bottom of a single cold leg. Each system was at its steady-state initial condition at the time of break initiation. The subsequent depressurization behavior was recorded for each facility and key data plots are presented herein for purposes of comparison. The vertical axis of each graph has been normalized as described previously. The APEX time scale has been multiplied by the scaling factor of two to compare with the SPES-2 time scale.

Figure 4 compares the APEX and SPES-2 pressure histories for the reactor vessel following the initiation of the simulated 2-inch cold leg break. As can be observed, the trends are very similar. Figures 5 through 8 present the data comparisons for the key passive safety systems.

In general, the data comparisons for the 2-inch break case indicate that the agreement between SPES-2 and APEX is very good. The timing of key events, such as ADS valve actuation, has been preserved.

VIII. CONCLUSIONS

This paper summarizes the rationale for scaling the depressurization behavior of fluids in phase equilibria. The key scaling groups are obtained by casting the depressurization rate equation in dimensionless form. Performing an order of magnitude analysis on the key scaling groups reveals that pressure scaling is complicated when Π_r exceeds unity. For the AP600 system, this occurs for breaks of approximately 2.5 cm or smaller.

Comparisons of the high pressure data from SPES-2 to the reduced pressure data from APEX indicate that pressure scaling can be successfully implemented in reduced pressure facilities.

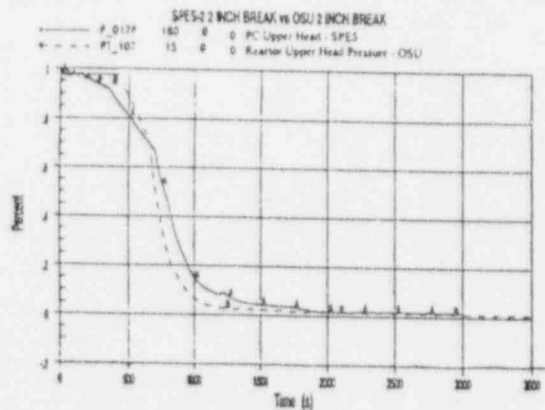


Figure 4. Comparison of OSU APEX and SPES-2 Two-Inch Break Pressure Histories

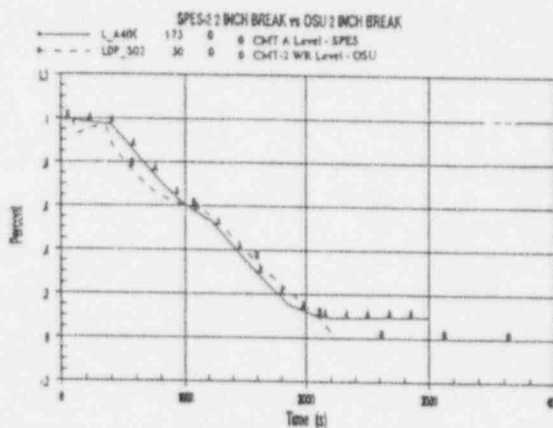


Figure 5. Comparison of OSU APEX and SPES-2 CMT-2 Liquid Level Histories

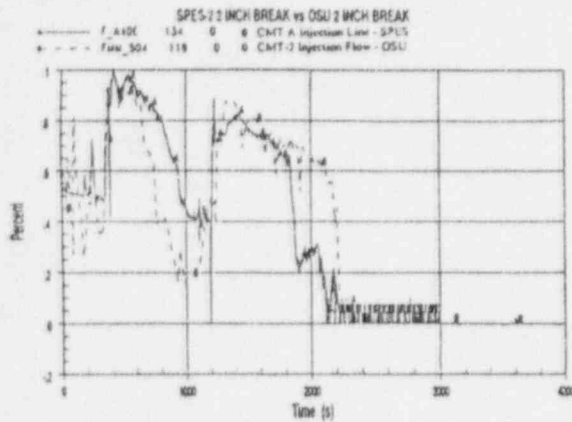


Figure 6. Comparison of OSU APEX and SPES-2 CMT-2 Injection Flow Rate

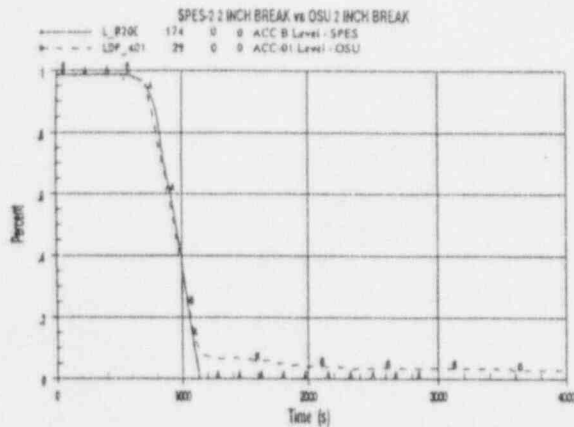


Figure 7. Comparison of OSU APEX and SPES-2 ACC-1 Liquid Level Histories

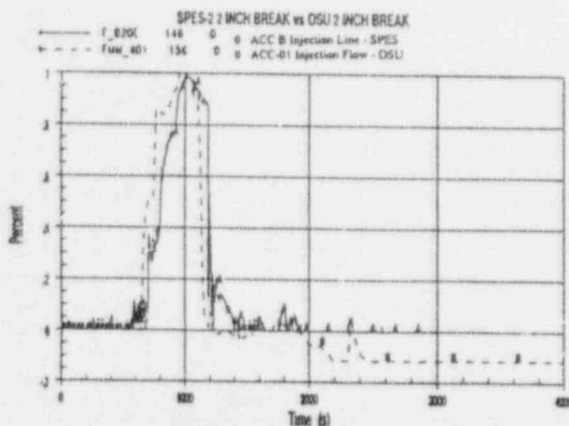


Figure 8. Comparison of OSU APEX and SPES-2 ACC-1 Injection Flow Rate

IX. REFERENCES

1. Reyes, J.N., Hochreiter, A.Y. Lafi, L.K. Lau, *Low Pressure Integral Systems Test at Oregon State University, Facility Scaling Report*, Westinghouse Electric Corporation, WCAP-14270, January 1995.
2. Zuber, N., "Appendix D: A Hierarchical, Two-Tiered Scaling Analysis," *An Integrated Structure and Scaling Methodology for Severe Accident Technical Issue Resolution*, U.S. Nuclear Regulatory Commission, Washington, DC 20555, NUREG/CR-5809, November 1991.
3. Henry, R.E. and H.K. Fauske. *The Two-phase Critical Flow of One-Component Mixtures in Nozzles, Orifices, and Short Tubes*, Journal of Heat Transfer, ASME Transactions, vol. 93, ser. C, no. 2, pp. 179-187, May 1971.
4. Briggs, John and F. David Peat. *Turbulent Mirror*. Harper & Row Publishers, New York, 1989.
5. Irey, R.K., Ansari, A., and Pohl, J.H., *Thermodynamics for Modular Instruction, Unit IC Properties of Pure Substances in Near Multiphase Regions*, John Wiley & Sons, New York, IC-35, 1967.
6. Keenan, J.H. Keyes, F.G., Hill, P.G., and Moore, J.G., *Steam Tables*, Wiley-Interscience, New York, 8-13, 1969.
7. Lay, J.F., *Statistical Mechanics and Thermodynamics of Matter*, Harper and Row Publishers, New York, 453-456, 1990.
8. Kocamustafaogullari, G., and Ishii, M., 1986. "Pressure and Fluid-to-Fluid Scaling Laws for Two-Phase Loop Flow," NUREG/CR-4585.
9. Hochreiter, L.E. and J.N. Reyes, "Comparison of SPES-2 and APEX Tests to Examine AP600 Integral System Performance," International Joint Power Generation Conference, Minneapolis, Minnesota, October 1995.